BULLETIN OF THE POLISH ACADEMY OF SCIENCES
TECHNICAL SCIENCES, Vol. 72(1), 2024, Article number: e148439
DOI: 10.24425/bpasts.2023.148439

POWER SYSTEMS AND POWER ELECTRONICS

Experimental study of dispersed flow in the thermopressor of the intercooling system for marine and stationary power plants compressors

Dmytro KONOVALOV [1], **Halina KOBALAVA** [2], **Mykola RADCHENKO** [3], **Terese LØVÅS** [1], **Anatoliy PAVLENKO** [4]*, **Roman RADCHENKO** [3], and **Andrii RADCHENKO** [3]

[1] Norwegian University of Science and Technology, Kolbjørn Hejes vei 1a, Trøndelag, Trondheim, 7034, Norway
[2] Admiral Makarov National University of Shipbuilding, Avenue Ushakov 44, Kherson, 73003, Ukraine
[3] Admiral Makarov National University of Shipbuilding, Machine Building Institute, Avenue 9, 54025 Mykolayiv, Ukraine
[4] Kielce University of Technology, Aleja Tysiąclecia Państwa Polskiego 7, Kielce, 25-314, Poland

Abstract. This study investigates the use of a thermopressor to achieve highly dispersed liquid atomization, with a primary focus on its application in enhancing contact cooling systems of the cyclic air for gas turbines. The use of a thermopressor results in a substantial reduction in the average droplet diameter, specifically to less than 25 μm, within the dispersed flow. Due to the practically instantaneous evaporation of highly atomized liquid droplets in accelerated superheated air, the pressure drop is reduced to a minimum. A further increase of the air pressure takes place in a diffuser. This allows for the compensation of hydraulic pressure losses in the air path, thereby reducing compressive work. Experimental data uncover a significant decrease in the average droplet diameter, with reductions ranging from 20 to 30 μm within the thermopressor due to increased flow turbulence and intense evaporation. The minimum achievable droplet diameter is as low as 15 μm and is accompanied by a notable increase in the fraction of small droplets (less than 25 μm) to 40-60%. Furthermore, the droplet distribution becomes more uniform, with the absence of large droplets exceeding 70 μm in diameter. Increasing the water flow during injection has a positive impact on the number of smaller droplets, particularly those around 25 μm, which is advantageous for contact cooling. The use of the thermopressor method for cooling cyclic air provides maximum protection to blade surfaces against drop-impact erosion, primarily due to the larger number of droplets with diameters below 25 μm. These findings underline the potential of a properly configured thermopressor to improve the efficiency of contact cooling systems in gas turbines, resulting in improved performance and reliability in power generation applications. The hydrodynamic principles explored in this study may have wide applications in marine and stationary power plants based on gas and steam turbines, and gas and internal combustion engines.

Keywords: energy efficiency; power plant; thermo-gas-dynamic effect; compressor; contact cooling.

1. INTRODUCTION

The utilization of modern power plants leads to an escalation in fuel consumption and the release of harmful substances into the environment [1, 2]. However, efforts to make heat engines greener contradict their energy efficiency, as emission reduction measures necessitate additional energy expenditures. The formation of nitrogen oxides (NOx) poses specific challenges, requiring the reduction of the maximum combustion temperature. Unfortunately, reducing this temperature also diminishes the fuel-energy efficiency of the engine. Consequently, there is an urgent need to develop technologies that are both environmentally friendly and energy efficient. These technologies should effectively minimize emissions while avoiding negative fuel and energy efficiency impacts [2, 3]. Over the past few decades, gas turbines and internal combustion engines have been extensively utilized as heat engines in shipbuilding and land-based energy systems. This popularity is due to their modular structures, adaptability to automation, high reliability and manufacturability, and relatively low investment costs [4, 5]. Gas turbines and internal combustion engines (diesel, gas piston engines, etc.) are used in autonomous power plants [6, 7], including plants of combined energy production (cogeneration and trigeneration) [8, 9] and transport energy plants [10, 11].

The fuel-energy efficiency of the engine largely depends on ambient parameters [12, 13]. As is known, when the air temperature increases, the fuel efficiency of engines decreases [14, 15]. For instance, the effect of higher turbine inlet air temperature by 1°C is a decrease in total power by approximately 0.7% [16, 17]. Therefore, developing and improving the technology for effective cool air in the gas turbine is a major task of modern energetics [18, 19].

There are several advanced directions, one of which is to ensure operation at a stabilized temperature level [20, 21] when using jet [22, 23] and absorption technologies [21, 24, 25]. At the same time, there are applied methods of thermodynamic and statistical analysis of the impact of various methods of cooling the cycle air and thermal load of engines of power plants [26,27].

*e-mail: apavlenko@tu.kielce.pl

Manuscript submitted 2023-07-17, revised 2023-10-26, initially accepted for publication 2023-11-07, published in February 2024.

These methods can be used to design heat recovery systems and thermophysical model processes to determine optimal operating modes [28, 29].

An interesting solution is the introduction of cycle air cooling technologies based on exhaust gas heat recovery [30, 31]. Air cooling can be used to improve the environmental friendliness of modern power plants [32,33], for example, in technologies based on water-fuel emulsions [34–36] and low-temperature condensation [37, 38]. However, the most common way to increase power and reduce fuel consumption is to use contact cooling of the airflow by water injection, which is characterized by a significant length of the evaporation zone and, consequently, power losses due to aerodynamic resistance [39–41]. The important thing to note is that it applies the system of the injected water using nozzles of different designs.

Contact cooling shows enormous potential in enhancing the efficiency of power plants that utilize gas turbine engines and internal combustion engines. This is achieved through the highly efficient cooling of the intermediate or charged air of the heat engine. Contact cooling also helps reduce hydraulic pressure losses in exhaust gas recirculation systems, further improving the efficiency of heat-utilizing refrigeration.

The next stage of improving such technology can be the use of a contact heat exchanger based on a thermo-gas-dynamic effect – thermopressor [42, 43]. A thermopressor is a two-phase jet apparatus spraying liquid in the airflow to cool it. It is necessary to organize the process of incomplete evaporation in its flow part to obtain a high-quality spray of water in the air stream by the thermopressor. On the one hand, it effectively cools the circulating air between the compressor stages of the gas turbine and reduces frictional losses in the thermopressor evaporative (working) chamber. On the other hand, this will allow obtaining a highly dispersed spray of water behind the diffuser of the thermopressor, that is, before the high-pressure compressor [44, 45]. Numerical (mathematical) modelling of processes in thermopressors does not allow us to fully determine the effectiveness of spraying water by the thermopressor due to the presence of complex intensive hydro-gas-dynamic and heat and mass transfer processes. The implementation of thermopressor technologies is limited by the insufficient availability of data from field tests, particularly concerning their integration into cooling systems [46, 47] and waste gas heat utilization systems [48, 49]. Additionally, the absence of comprehensive mathematical and physical models for the working processes of thermopressors hinders the development of rational methods for organizing thermophysical cooling processes. Furthermore, there is a need for methodologies that facilitate the rational design [50, 51] and determination of optimal parameters [52, 53], ensuring maximum improvements in power and efficiency while reducing specific fuel consumption in power plants.

Therefore, an experimental study, followed by clarifying components for numerical modelling, is more appropriate and will allow us to determine the optimal parameters of the resulting dispersed flow: the distribution of temperatures, concentrations of mixture components, heat fluxes, and masses of a dispersed high-velocity flow.

2. LITERATURE REVIEW

The achievement of high-quality organization of highly dispersed and uniform spraying of injected water is the main issue for the development of the injection system. The water supply to the compressor air path is accompanied by the appearance of consequent problems with the feature of gas turbine operation:

1. Insufficient quality of the spraying can allow liquid film on the blade surface of the compressor.
2. Insufficient intensive water evaporation of large droplets from the surface and as a result, the cooling efficiency of the airflow decreases.
3. Losses due to droplets friction in the flow when it accelerates up to flow velocity, as well as friction, liquid films on the surface of the blades, and the compressor housing. As a result, the internal efficiency of the stages and the compressor decreases.
4. Appearing drip-impact erosion on the surface of the compressor blades.

A good method for solving problems presented before is the achievement of dispersion flow quality. This requires the implementation of injection technologies that make it possible to provide fine atomization of the injected water in the form of a mist [54, 55]. The efficiency of "wet" compression primarily depends on the intensity of evaporation and heat exchange of droplets with the airflow [56, 57], which begins to increase sharply with a decrease in the effective droplet diameter to 3 μm [16,58]. This happens as a result of a significant increase in the total surface area of the droplets, which, in turn, is inversely proportional to their average diameter. However, modern mechanical and pneumatic nozzles do not allow spraying water with an effective droplet diameter of less than 30 μm [59, 60].

One method to achieve more efficient atomization is to use a liquid that is super-heated relative to its saturation temperature. In the process of injection of such a liquid through the nozzle of a spraying device, its explosive boiling occurs, as a result of which the liquid is crushed into small particles [61–65].

Among the last publications [66, 67], there is a rather unusual solution to the spraying problem proposed by Mee Industries Inc. [68, 69]. To supply water to the airflow, nozzles of a distinctive design have been developed (the diameter of the outlet is 0.1–0.4 mm), in which spraying is realized due to impact action. Water under high pressure (7–14 MPa) is supplied to the nozzle head, after which it is broken, thanks to the "pin", into small droplets, the diameter of which does not exceed 30 μm [70, 71]. According to Mee Industries Inc., the increase in the efficiency of gas turbines using a contact cooling system in the summer reaches 2–4%. Despite the relatively wide distribution of such systems, they require rather complex pumping equipment for water supply and create certain difficulties when operating the system under high pressure [68, 72].

A promising direction is the implementation of TOPHAT technology (Alpha Power Systems). Its essence lies in the injection of water superheated at saturation temperature through centrifugal nozzles to the compressor inlet. When water leaves the nozzle duct, the liquid boils instantaneously, as a result of which the flow breaks up into smaller droplets [73, 74]. Using such technology makes it possible to obtain a high efficiency of a gas turbine (57.4%). It was experimentally established that if the diameter of a water droplet in the flow part of the compressor did not exceed 10 μm, then the effect of centrifugal forces on the droplet became almost imperceptible and the droplets moved along the airflow. At the same time, the optimal flow has the average size of droplets no more than 20–25 μm at the compressor inlet [75, 76]. It was found that with the injection of superheated water at 220–240°C and pressure in front of the nozzle of 4–8 MPa, it was possible to provide the necessary fine atomization: 65–70% of the droplets by weight to a diameter in the range of 0.2–3.0 μm [77]. Experiments to determine the disperse characteristics of the air-droplet flow showed that the distribution and the speed of droplet expansion were primarily determined not by the design of the nozzle, but by the "explosive" formation of droplets in the process of intensive generation of the vapor phase at the nozzle outlet [78,79]. The implementation of the contact cooling process requires substantial amounts of water, since the cooling water in the form of steam, together with the exhaust gases, is released into the environment. To avoid salt deposits on compressor parts, humidification of cycle air must be conducted with well-purified water. This, in turn, leads to significant expenditures for water treatment [80]. However, if the water supplied to the compressor is separated at the outlet of the unit, for example, by condensing it from the exhaust gases, as is done in Aquarius-type plants, then this drawback is eliminated. In this case, the problem of increasing the efficiency of a power plant by approaching the process of compressing air to isothermal in the GTE compressor by injection of cooling water passes to real technical use.

The analysis of the considered technologies for evaporative contact inter-cooling of gas turbine cyclic air proves the feasibility of using these systems to improve the performance and reliability of combustion engines: gas turbines [81] and gas engines [82], internal combustion engines [83], as well as engine cyclic air and space air condition systems in stationary [84] and transport [85] applications.

One of the advanced technologies in this direction is the use of a thermopressor, whose operation is based on realizing thermo-gas-dynamic compression [86]. This effect appears in the evaporation process of the high-dispersion liquid in the airflow moving with transonic velocity but not exceeding it. At the same time, air temperature is decreasing with a simultaneous increase in the total pressure. The temperatures of air supplied between the inlet and outlet of the thermopressor are reduced, which is caused by removing the heat from the air for evaporation of liquid injected into the airstream. In the well-profiled nozzle of a real thermopressor, the expansion occurs practically adiabatically. In the narrow part of the nozzle, the airflow moves at a speed of (0.5...0.9)M, and mechanically atomized water is injected. Their interaction in the evaporation chamber is accompanied by the acceleration of the flow due to the evaporation of droplets. Because of the practically instantaneous evaporation of liquid droplets in accelerated superheated air, the pressure drop is reduced to a minimum. A further increase of the air pressure takes place in a diffuser. Due to instantaneous evaporation of highly dispersed liquid, not only a significant reduction in resistance but also an increase in the total pressure in the air stream becomes possible. It should be noted that the quality of liquid atomization, that is the diameter of the water drop, affects the length of the evaporation section and the velocity regime of the apparatus [87, 88] and the decrease in the primary drop size and the length of the evaporation section largely impact the reduction of friction losses [89]. Hence, using thermopressor allows for providing cooling air simultaneously with obtaining smaller droplets of the outlet. The optimal solution is the installed thermopressor between the stages of the gas turbine. This is because air temperature between compressor stages can be high enough (up to 180°C and more), which provides intensive evaporation of water droplets. However, to check the opportunity of making flow with droplets diameter lower than the maximum for use in the gas turbine, it is necessary to conduct experimental research to determine the influence characteristics and use conditions of the thermopressor on the flow dispersion quality.

Thermopressor technologies are particularly well-suited for the integration into heat utilization circuits in power plants, especially in the context of economic development in European countries and post-war Ukraine. These technologies offer substantial advantages over traditional methods and deep heat utilization techniques, resulting in greater fuel efficiency and increased power generation.

Internal combustion engines and gas turbines used in stationary and marine power plants are key sectors where these technologies can be applied. By implementing thermopressor technologies, significant reductions in fuel consumption can be achieved, leading to enhanced energy security levels.

3. MATERIALS AND METHODS

The experimental thermopressor (Fig. 1) consists of a receiving chamber; confuser; evaporation chambers; diffuser; and section for installing measuring pressure and temperature sensors. The evaporation chamber of the thermopressor is made in several variations, which in turn made it possible to conduct research with different geometric characteristics (Table 1). Also experimental setup including drive electric motor (55 kW, 2950 rpm), air receiver (Atlas Copco), compressor (XA 85, Atlas Copco), oil cooler, air filters (4N-0015 CAT), oil receiver (Atlas Copco), air dehumidifier of the "Cyclone" type (Ø 700 × 1060), oil-wet separator (CAF-3), catcher of water drops for obtaining samples (exposure time when taking samples – 1.0; 2.0 s), pressure control valve, high-pressure pump for water supply (STIHL RE 98, pressure up to 11 MPa), distilled water storage tank ($V = 50$ liters).

For water injection, nozzles of the "fog" type were used. The nozzles provided the following values of water flow at the inlet to the receiving chamber of the thermopressor (pressure 7.5 MPa): #1 – $G_w = 0.0175$ kg/s; #2 – $G_w = 0.0407$ kg/s; #3 – $G_w = 0.0487$ kg/s. In this case, the water spray angle was 70–90° and the average droplet diameter in the dispersed flow was $\delta_w = 40-60$ μm, with the maximum diameter being $\delta_w > 100$ μm. For visual registration and measurement of the dispersion of water droplets in different parts of the flow part of

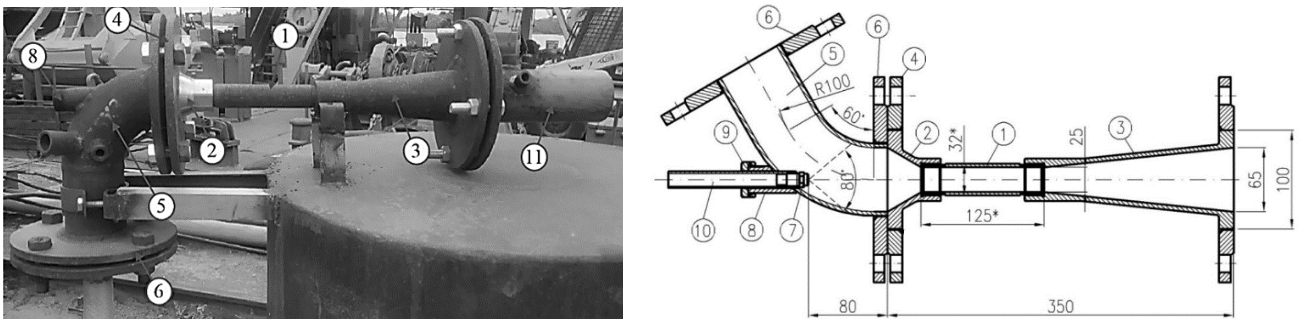

(a) (b)

Fig. 1. Experimental thermopressor (photo (a) and sketch (b)): 1 – evaporation chamber; 2 – confuser; 3 – diffuser; 4, 6 – flanges; 5 – receiving chamber; 7 – nozzle; 8 – section for installing nozzle; 9 – regulation nut; 10 – water supply tube; 11 – nozzle for installing sensors

Table 1
Geometrical parameters of the experimental thermopressor

Parameter	Value
The length of the thermopressor L_{tp}, mm	387
Receiving chamber	
Diameter D_1, mm	65
Length L_1, mm	200
Confuser	
Input diameter D_{c1}, mm	65
Output diameter D_{c2}, mm	25
The corner of the confuser α_c, °	30
Length L_c, mm ($\alpha_c = 30°$)	34
Diffuser	
Input diameter D_{d1}, mm	25
Output diameter D_{d2}, mm	65
Taper angle for the diffuser β_d, °	5
Length L_d, mm ($\beta d = 5°$)	228
Evaporation chamber with (L/D) = 5	
Diameter D_{ch}, mm	25
Length L_{ch}, mm	125, 175
Nozzles: #1 – $G_w = 0.0175$ kg/s; #2 – $G_w = 0.0407$ kg/s; #3 – $G_w = 0.0487$ kg/s	
The distance between the point of water exit to the entrance to the evaporation chamber L_f, mm	125
Discharge nozzle of the thermopressor	
Diameter D_2, mm	65
Length L_2, mm	200

the thermopressor, an optical microscope USB Digital Microscope with high readout capability and electronic measurement system was used with a magnification factor of 10× ~300× and a computerized system for photographing and determining the diameter of droplets with a measurement accuracy of 1 μm. The flow dispersion in various parts of the thermopressor flow part was determined as a result of sampling by trapping droplets from the airflow into the immersion medium. After that, the droplet size was measured using a microscope with a digital camera installed. Before the experiment, the microscope measuring system was calibrated and checked for accuracy and measurement range.

Droplets were captured using a specially designed device based on the shutter mechanism of a camera with a shutter speed of 1 and 2 s. The glass slide was covered with a thin layer of 0.5–1.0 mm thick viscous liquid. Droplets of water that fell on the glass did not dissolve, did not evaporate, and did not coagulate for up to 2 minutes, which is sufficient for a photo and video recording of the sample and subsequent processing to determine the size and number of droplets.

As an immersion medium, mixtures of motor oil and lithol were used in a ratio of 2.5:1.0. The choice of the immersion medium was made based on the necessary conditions of the experiment.

Usually, air coolers are installed between the compressor stages of the gas turbine (Fig. 2a). The operation conditions of the thermopressor are installed according to a similar principle, which is between the low (LPC) and high-pressure compressors (HPC) of the gas turbine installation (Fig. 2b) instead of a surface or contact air cooler. At the same time, water is supplied from a freshwater storage tank by a high-pressure pump.

It should be noted that to evaluate the precision of measurements in experimental research, it is crucial to ascertain the measurement error. This error is influenced by several factors, including the errors of measuring devices, methodological errors, and systematic errors. The process of measuring a specific quantity involves selecting the measurement method, utilizing appropriate measuring instruments, and determining the method of recording the acquired results. The absolute measurement error is calculated as the sum of the methodological error, instrumental error, and observational error. The overall measurement error is determined by the total values of all components within the information and measurement system. Each of these components possesses its own distinctive values for methodical, instrumental, systematic, or random errors.

During the experiment, the measurement uncertainty arises from both methodological errors and inaccuracies in the measuring devices, contributing to the systematic error component. To assess the accuracy of measurement outcomes, the Student

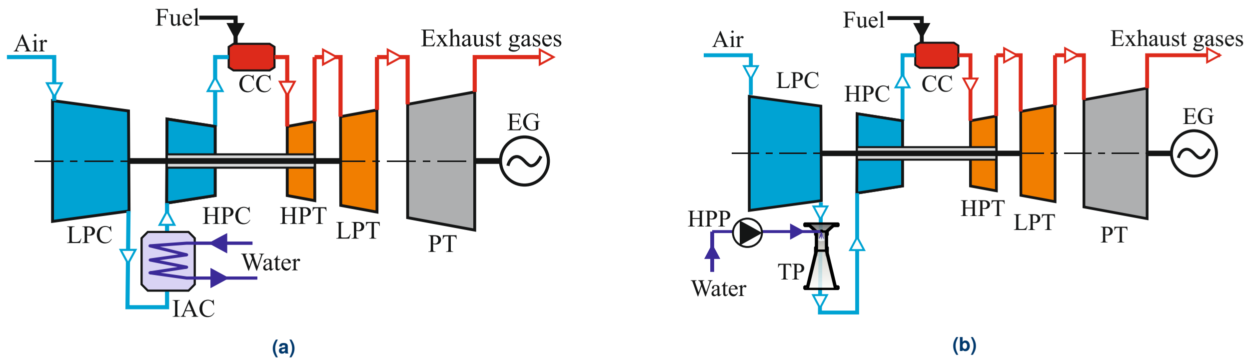

Fig. 2. Gas turbine schemes with inter-cooling between compressor stages: (a) a scheme with inter-cooling by heat exchanger; (b) a scheme with inter-cooling by a thermopressor; LPC – low-pressure compressor; HPC – high-pressure compressor; CC – combustion chamber; HPT – high-pressure turbine; LPT – low-pressure turbine; PT – power turbine; HPP – high-pressure pump; EG electric generator; IAC – intermediate air cooler; TP – thermopressor

method was used, especially suitable when the number of observations is limited to $n \leq 20$. Moreover, it is assumed that the distribution of uncertainty in each measurement follows a normal distribution. The determination of the quantile value in this distribution depends on the confidence probability, which was set at $P = 0.95$. In accordance with the presented methodology, the uncertainties of measuring were calculated (Table 2). At the same time, the maximum measurement uncertainty was ±7.62%.

Table 2
The maximum measurement uncertainty

Pressure increase in the thermopressor $\varepsilon_{tp} = n_2/n_1$	Mean square deviation σ	Quantile distribution $t_{p=0.95}$	Confidence value of the error $\Delta_{0.95}$	Measurement uncertainty δ_{tp} %
Relative air velocity in the evaporation chamber $w_{a1} = 0.3$–0.6 Ma; Inlet air temperature $p_{a1} = 423$ K; Relative water consumption $g_w = 3$–20%				
Nozzle #1				
1.0354	0.00847	12.7062	0.07611	7.35
1.0285	0.00762	12.7062	0.06841	6.65
1.0253	0.00139	4.3027	0.00345	0.34
0.9707	0.01395	2.7764	0.01735	1.79
0.9611	0.03617	2.5706	0.04106	4.27
Nozzle #2				
0.9964	0.00175	4.3027	0.00435	0.44
0.9660	0.00820	12.7062	0.07364	7.62
0.9734	0.01297	3.1824	0.02063	2.12
0.9494	0.00001	12.7062	0.00001	0.01
0.9341	0.00306	2.7764	0.00381	0.41
0.9251	0.04413	2.2622	0.03154	3.41
Nozzle #3				
0.9982	0.01281	4.3027	0.03181	3.35
0.9485	0.01103	4.3027	0.02738	3.02
0.9081	0.00001	12.7062	0.00001	0.01
0.8895	0.00179	3.1824	0.00285	0.32
0.8802	0.02073	2.7764	0.02578	2.97
0.8668	0.01467	2.7764	0.01824	2.14
0.8533	0.00284	4.3027	0.00706	0.85
0.8286	0.01281	4.3027	0.03181	3.35

4. RESULTS AND DISCUSSION

A crucial factor affecting the efficiency of using a thermopressor as a means of highly dispersed liquid atomization is the influence of working processes in its flow part on dispersion (average diameter and number of droplets). The smaller the average diameter and the smaller the distribution range of these droplets (the greater the number of small droplets), the more efficient it will be to ensure the isothermal process in subsequent compressor stages.

It is necessary to compare the results of measuring the droplet diameter in a working apparatus with the droplet diameters supplied with a nozzle at the outlet to determine the efficiency of droplet crushing and reduction of their diameter due to partial evaporation.

In the first stage of the study, the droplet diameter of three nozzles with different water flow rates was measured. The liquid pressure during the experiment at the nozzle inlet was 7.5–8.0 MPa, which ensured this type of the smallest possible droplet diameter of the nozzle.

The results obtained by injecting liquid through the nozzles at a pressure of 7.5 MPa are shown in Figs. 3a–3c. It can be seen that the diameter of the droplets in the dispersed flow is 25–110 µm. At the same time, it should be noted that the distribution of drops is quite unequal. The number of small drops with a diameter of 25–40 µm is 25-40% with a relative mass of 5–10%. The distribution shifts in the direction of an increase in the drop diameter, and a large number of drops with a diameter of 80–110 µm appear with an increase in water consumption. It should be noted that the distribution of droplets, in this case, is unequal, and almost 60% of the droplets reach a diameter of 70–80 µm, and there are droplets of 100 µm, which greatly complicates the evaporation of the liquid in the flow part of the compressor.

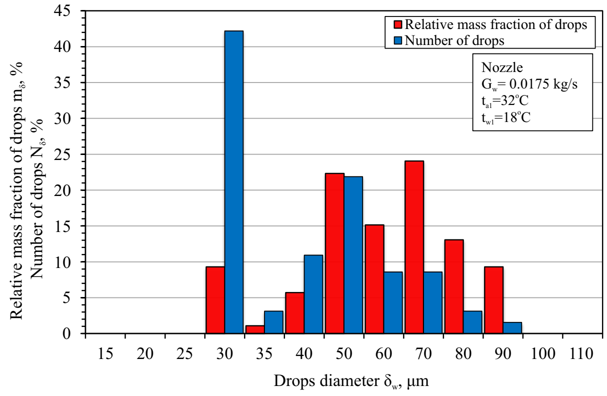
Relative mass fraction of drops
Number of drops
Nozzle
G_w = 0.0175 kg/s
t_{a1}=32°C
t_{w1}=18°C
Relative mass fraction of drops $m_δ$, %
Number of drops $N_δ$, %
Drops diameter $δ_w$, μm

(a)

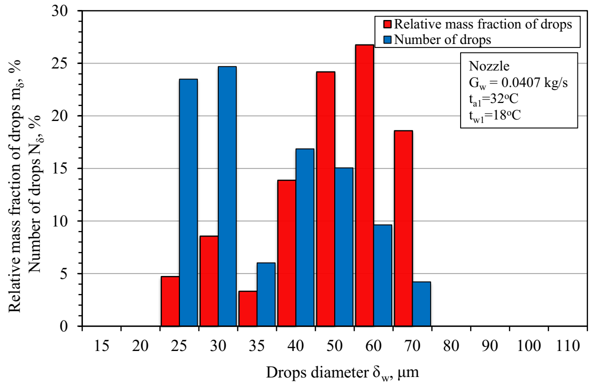
Relative mass fraction of drops
Number of drops
Nozzle
G_w = 0.0407 kg/s
t_{a1}=32°C
t_{w1}=18°C
Relative mass fraction of drops $m_δ$, %
Number of drops $N_δ$, %
Drops diameter $δ_w$, μm

(b)

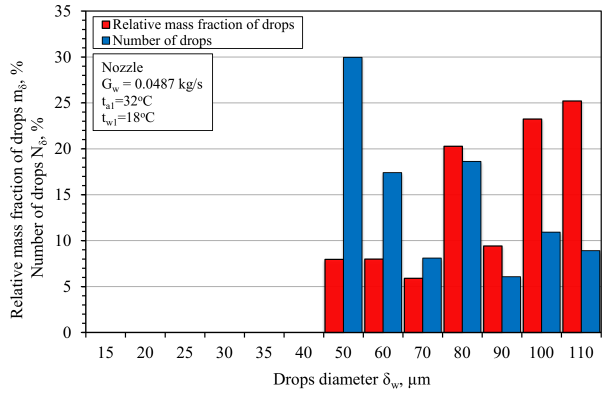
Relative mass fraction of drops
Number of drops
Nozzle
G_w = 0.0487 kg/s
t_{a1}=32°C
t_{w1}=18°C
Relative mass fraction of drops $m_δ$, %
Number of drops $N_δ$, %
Drops diameter $δ_w$, μm

(c)

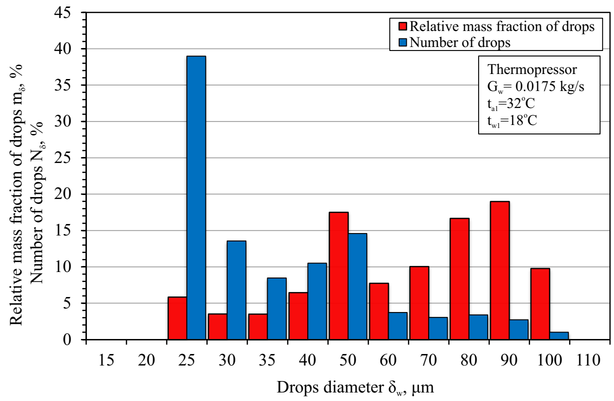
Relative mass fraction of drops
Number of drops
Thermopressor
G_w = 0.0175 kg/s
t_{a1}=32°C
t_{w1}=18°C
Relative mass fraction of drops $m_δ$, %
Number of drops $N_δ$, %
Drops diameter $δ_w$, μm

(d)

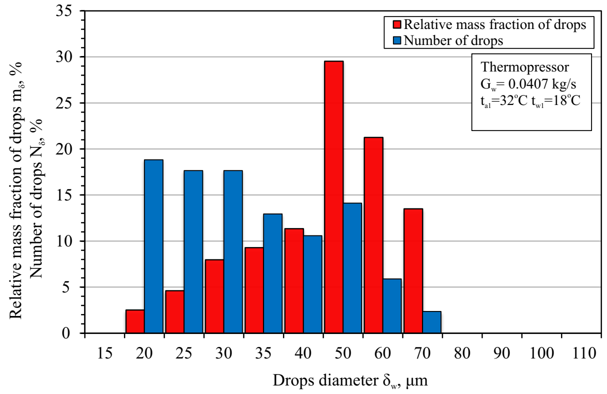
Relative mass fraction of drops
Number of drops
Thermopressor
G_w = 0.0407 kg/s
t_{a1}=32°C t_{w1}=18°C
Relative mass fraction of drops $m_δ$, %
Number of drops $N_δ$, %
Drops diameter $δ_w$, μm

(e)

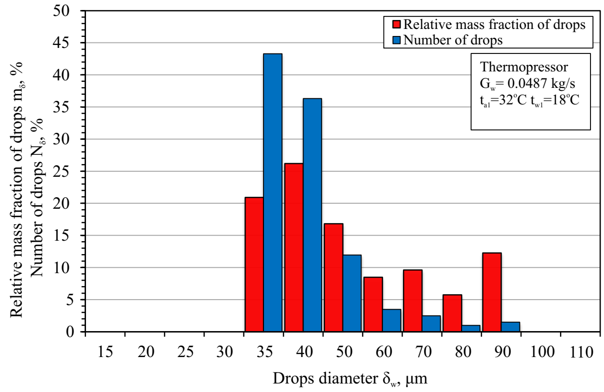
Relative mass fraction of drops
Number of drops
Thermopressor
G_w = 0.0487 kg/s
t_{a1}=32°C t_{w1}=18°C
Relative mass fraction of drops $m_δ$, %
Number of drops $N_δ$, %
Drops diameter $δ_w$, μm

(f)

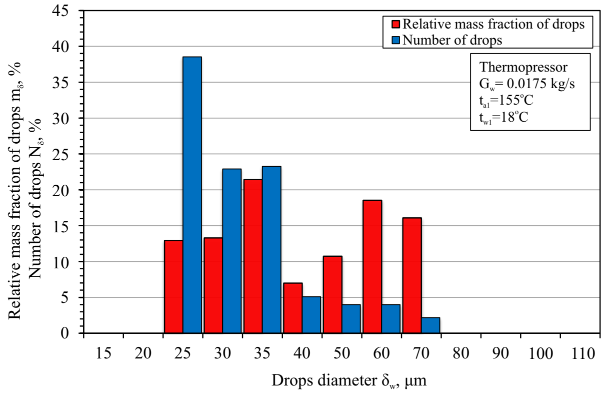
Relative mass fraction of drops
Number of drops
Thermopressor
G_w = 0.0175 kg/s
t_{a1}=155°C
t_{w1}=18°C
Relative mass fraction of drops $m_δ$, %
Number of drops $N_δ$, %
Drops diameter $δ_w$, μm

(g)

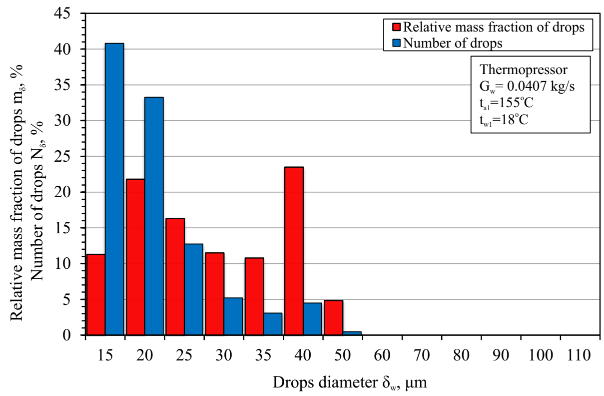
Relative mass fraction of drops
Number of drops
Thermopressor
G_w = 0.0407 kg/s
t_{a1}=155°C
t_{w1}=18°C
Relative mass fraction of drops $m_δ$, %
Number of drops $N_δ$, %
Drops diameter $δ_w$, μm

(h)

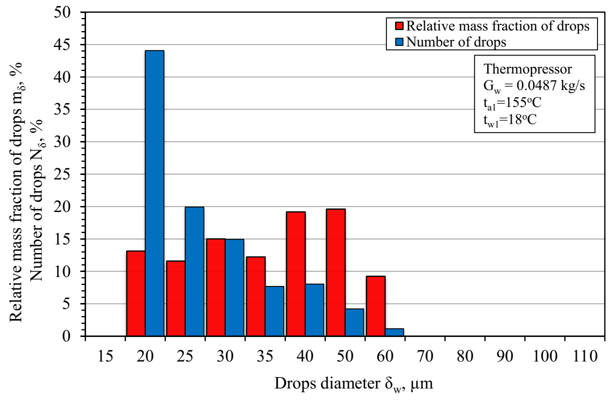

(i)

Fig. 3. Distribution of droplets by groups of diameters with a flow rate of injected water: nozzle (a, b, c), thermopressor without evaporation (d, e, f), thermopressor with incomplete evaporation (g, h, i)

In the second stage of the study, droplets were measured in a dispersed flow at the outlet of the thermopressor flow part during operation without evaporation of droplets, that is, in cold air (Figs. 3d–3f). It can be seen that a larger number of small drops with a diameter of 25–45 µm are formed. At the same time, the total amount for all three types of nozzles is 60–75% (20–30% by relative weight). However, the number of droplets with a diameter of less than 25 µm is less than 40% (10% by mass). When the water flow rate increases, the number of small drops decreases and, for example, for nozzle # 3 with a flow rate of 0.0487 kg/s, there are no drops with a diameter of less than 35 µm.

A larger number of small drops with a diameter of 25–45 microns are formed. At the same time, the total amount for all three types of nozzles is 60–75% (20–30% by relative weight). However, the number of droplets with a diameter of less than 25 µm is less than 40% (10% by mass). When the water flow rate increases, the number of small drops decreases and, for example, for nozzle #3 with a flow rate of 0.0487 kg/s, there are no drops with a diameter of less than 35 µm. The change in droplet diameter distribution relative to an injection without a thermopressor is explained by the high flow rate and, as a result, additional intense turbulence. However, at the same time, you can see a sufficient number of large drops with a diameter above 60 µm is 15–20% (35–50% by mass).

The turbulence of the flow in the thermopressor flow path positively affected the average diameter of the droplets at the outlet. It decreased by 5 µm, and for a nozzle #3, the diameter decreased even up to 30 µm is observed. It should also be noted that large droplets above 60 µm have not been a positive development for the method for injecting liquid between compressor stages.

At the third stage of the study, the characteristics of the dispersed flow were studied in the presence of the evaporation process in the flow part of the thermopressor (Figs. 3g–3i). The injection was made into an airflow with a temperature of 155°C. After cooling at the thermopressor outlet, the air temperature varied within 30–45°C. The flow rate in the evaporation chamber reached $M = 0.35-0.80$. It can be seen that the number of small droplets increases and amounts to 80–90% (40–55% by mass) with a diameter of less than 35 µm. When using nozzle #2, drops with a diameter of 15 µm are collected. The share of droplets with a diameter greater than 60 µm decreases significantly and amounts to 2–5% (10–30% by mass). Droplets with a diameter greater than 70 µm are not observed.

Figure 4 shows photos of droplet samples for all three types of nozzles. The distribution of drops across the cross-section of the flow part of the thermopressor is quite uniform, and there are also no large-sized drops with a diameter of 100 µm or more. The number and diameter of drops closer to the walls of the thermopressor increases. This may indicate the need to determine the optimal parameters of the jet of injected water to ensure a more effective distribution of drops across the cross-section of the flow part.

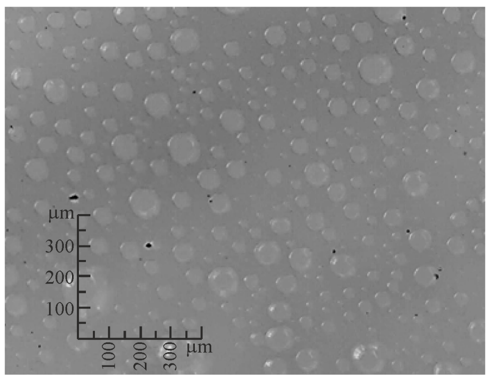

(a)

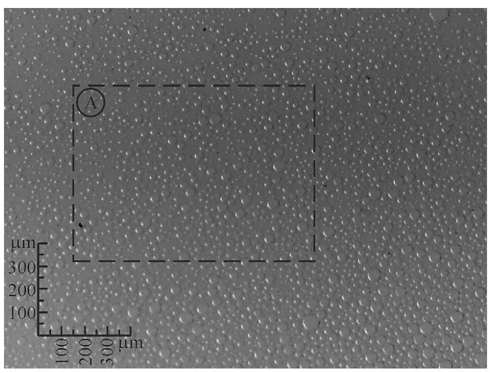

(b)

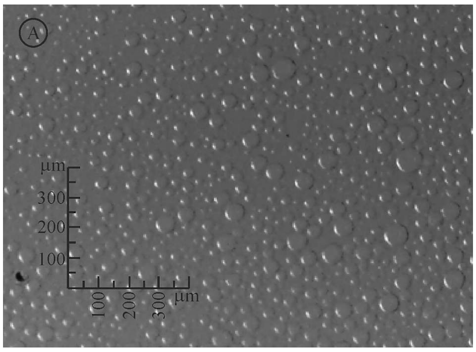

(c)

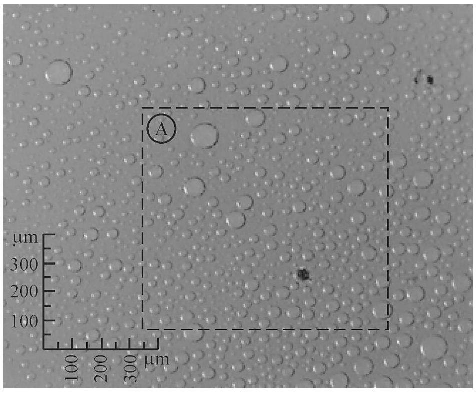

(d)

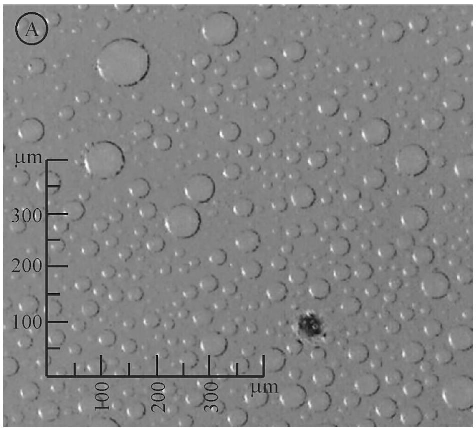

(e)

Fig. 4. Photo of captured droplets (thermopressor with evaporation) for nozzles: #1 – $G_w = 0.0175$ kg/s (a); #2 – $G_w = 0.0407$ kg/s (b, c); #3 – $G_w = 0.0487$ kg/s (d, e)

Summarizing the results of measurements of droplet diameters with different water flow rates, as well as with and without the presence of evaporation in the thermopressor flow path, it can be said that in the thermopressor, the average droplet diameter is significantly reduced due to the high turbulence of the flow and the process of intensive evaporation in the flow with high temperature. The minimum achievable droplet diameter is 15 µm (it decreases in the thermopressor flow part by 15–30 µm on average), and at the same time, the proportion of small droplets (less than 20 µm) has increased, which is 20–40% (compared to the basic values of 3–20%). In addition, the droplet diameter distribution is more even, and there are no large droplets with a diameter above 70 µm. In the measured airflow, a certain number of smaller droplets (less than 10–15 µm) exist. However, due to the complexity of the experiment, the measurement of this quality is adequate only when using a special measuring tool.

In order to evaluate the efficiency of using a thermopressor as a device for obtaining a highly dispersed flow, a comparative analysis of the dispersed flow quality under different injection conditions should be made with the water flow rate at the inlet (nozzle type). The analysis of the drop distribution by diameter groups for a nozzle with a flow rate of 0.0175 kg/s (nozzle #1) is shown in Figs. 5a–5d). The use of a thermopressor with incomplete evaporation makes it possible to reduce the diameter of drops with the maximum relative mass by 35 µm (Fig. 5a) and will be 35 µm. At the same time, the value of the relative mass practically does not change and is about 21–24%. The diameter of the drops with the maximum number decreases by 5 µm (Fig. 5b), and with a diameter of 25 µm, it corresponds to 39% of the total number of drops and a relative mass of 12.9% (Fig. 5c). The drops share with a diameter of less than 35 µm increases to 85%, and there are no drops with a diameter of more than 70 µm (Fig. 5d), which is a satisfactory result.

The increase in water consumption during injection (nozzle #2) shows a similar dependence when using incomplete

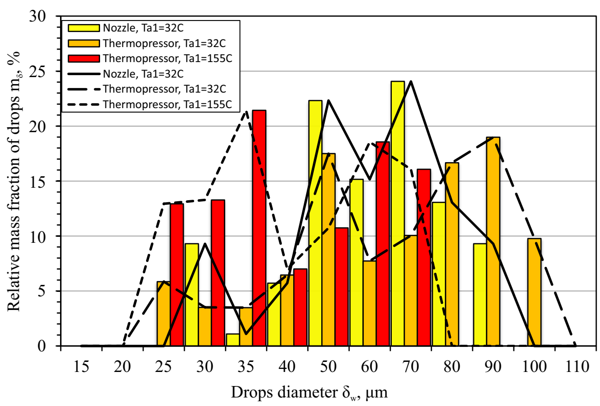

(a)

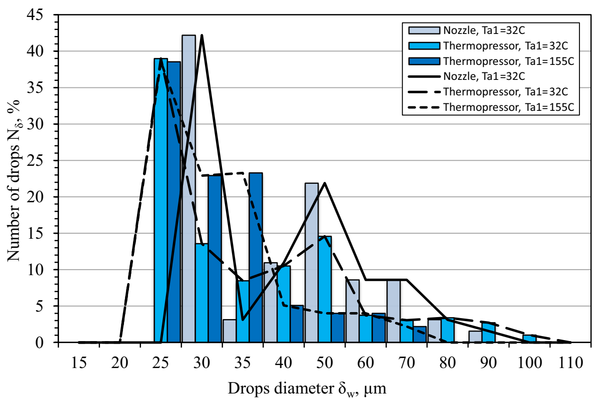

(b)

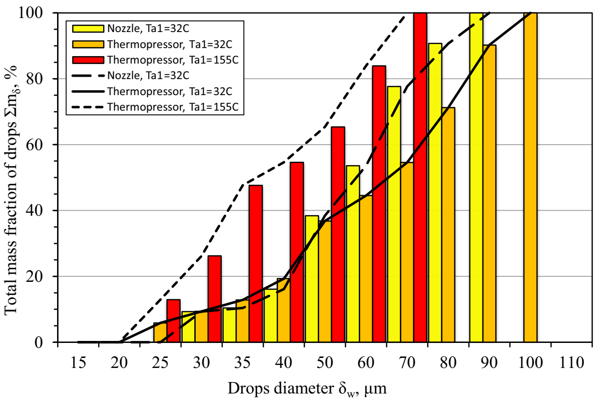
Total mass fraction of drops Σm$_δ$, %
Drops diameter δ$_w$, μm
Nozzle, Ta1=32C
Thermopressor, Ta1=32C
Thermopressor, Ta1=155C
Nozzle, Ta1=32C
Thermopressor, Ta1=32C
Thermopressor, Ta1=155C

(c)

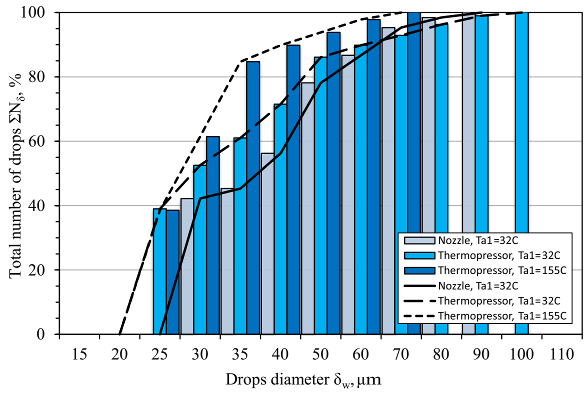
Total number of drops ΣN$_δ$, %
Drops diameter δ$_w$, μm
Nozzle, Ta1=32C
Thermopressor, Ta1=32C
Thermopressor, Ta1=155C
Nozzle, Ta1=32C
Thermopressor, Ta1=32C
Thermopressor, Ta1=155C

(d)

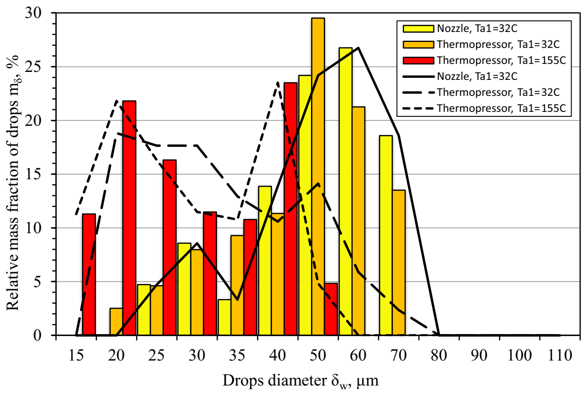
Relative mass fraction of drops m$_δ$, %
Drops diameter δ$_w$, μm
Nozzle, Ta1=32C
Thermopressor, Ta1=32C
Thermopressor, Ta1=155C
Nozzle, Ta1=32C
Thermopressor, Ta1=32C
Thermopressor, Ta1=155C

(e)

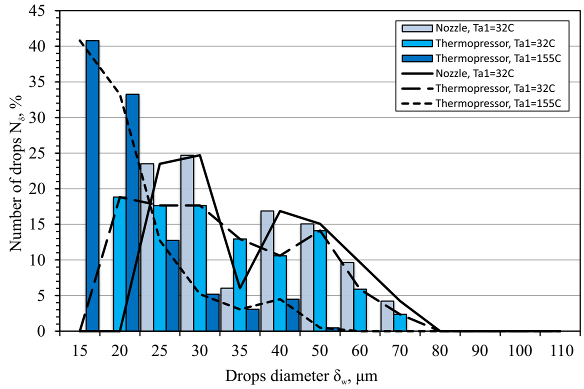
Number of drops N$_δ$, %
Drops diameter δ$_w$, μm
Nozzle, Ta1=32C
Thermopressor, Ta1=32C
Thermopressor, Ta1=155C
Nozzle, Ta1=32C
Thermopressor, Ta1=32C
Thermopressor, Ta1=155C

(f)

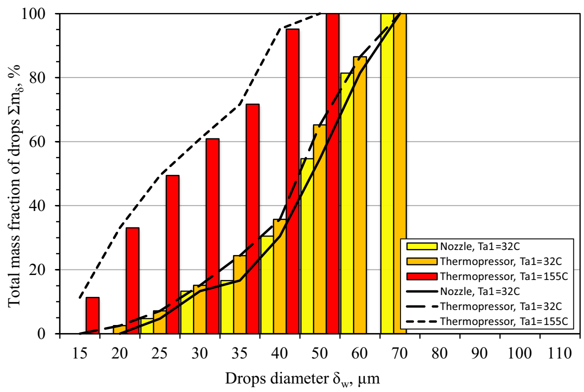
Total mass fraction of drops Σm$_δ$, %
Drops diameter δ$_w$, μm
Nozzle, Ta1=32C
Thermopressor, Ta1=32C
Thermopressor, Ta1=155C
Nozzle, Ta1=32C
Thermopressor, Ta1=32C
Thermopressor, Ta1=155C

(g)

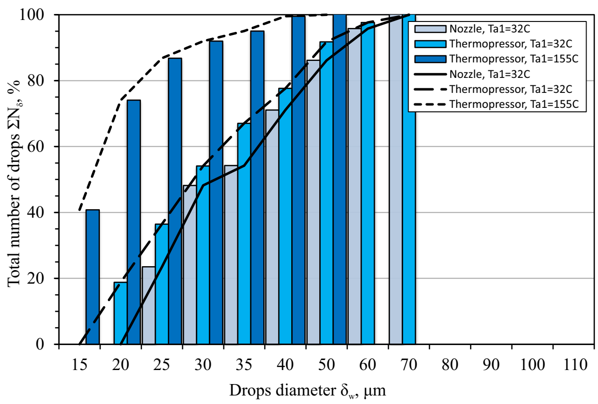
Total number of drops ΣN$_δ$, %
Drops diameter δ$_w$, μm
Nozzle, Ta1=32C
Thermopressor, Ta1=32C
Thermopressor, Ta1=155C
Nozzle, Ta1=32C
Thermopressor, Ta1=32C
Thermopressor, Ta1=155C

(h)

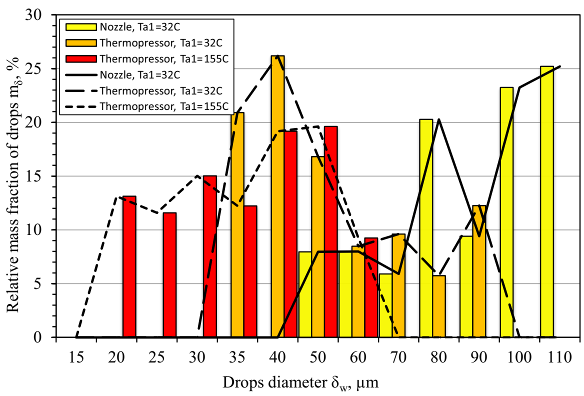
Relative mass fraction of drops m$_δ$, %
Drops diameter δ$_w$, μm
Nozzle, Ta1=32C
Thermopressor, Ta1=32C
Thermopressor, Ta1=155C
Nozzle, Ta1=32C
Thermopressor, Ta1=32C
Thermopressor, Ta1=155C

(i)

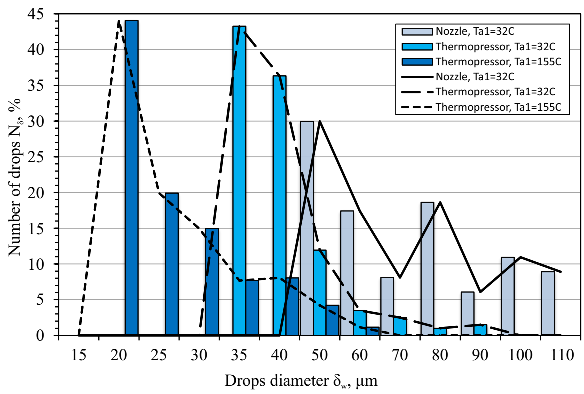
Number of drops N$_δ$, %
Drops diameter δ$_w$, μm
Nozzle, Ta1=32C
Thermopressor, Ta1=32C
Thermopressor, Ta1=155C
Nozzle, Ta1=32C
Thermopressor, Ta1=32C
Thermopressor, Ta1=155C

(j)

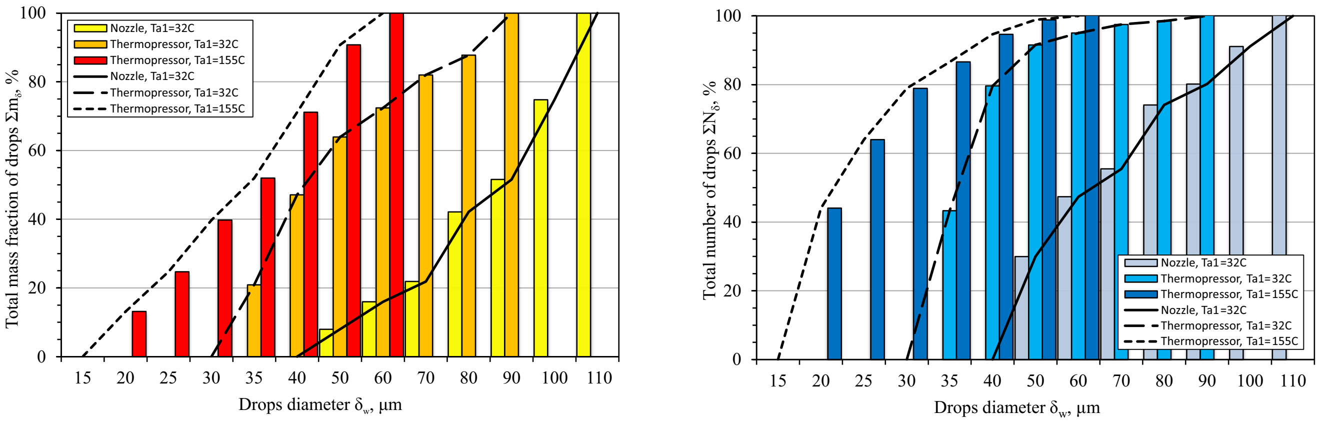

(k) (l)

Fig. 5. Comparison of droplet distribution by groups of diameters for the flow rate of injected water: G_w = 0.0175 kg/s (a–d), 0.0407 kg/s (e–h), 0.0487 kg/s (i–l)

evaporation (Figs. 5e–5h). At the same time, the diameter with the maximum relative mass decreases from 60 μm to 20 μm (Fig. 5e). Drops with a diameter of 15 μm appear, the number of which is about 40% (Fig. 5f). The relative weight of drops with a diameter less than 25 μm is 49.4% (Fig. 5g) with a size of 86.8% (Fig. 5h), which is the best result obtained during the experiment.

The study of a thermopressor with incomplete evaporation when using nozzle #3 with a flow rate of 0.0487 kg/s shows that an increase in water flow during injection does not affect the quality of obtaining a dispersed flow. At the same time, the number of large drops in the flow is significantly reduced. The maximum drop diameter decreases from 110 μm to 60 μm (Fig. 5i). Their relative weight is less than 10%, and the number does not exceed 1–2% (Fig. 5j). However, drops with a diameter of 40 μm make up the largest share by mass – 18%. Droplets with a diameter of 25 μm by mass are 24.7% (Fig. 5k), with a considerable number of them – 64% (Fig. 5l), which is a satisfactory result with the quality of the dispersed flow.

Analyzing the experimental data, the following can be stated. Increasing water flow during injection has a positive effect on increasing the number of drops with a diameter of 25 μm, which is most beneficial for contact cooling (nozzle #3). However, the maximum relative weight of such drops is observed for nozzle #2. A similar conclusion can be drawn by analyzing the value of the average droplet diameter of the dispersed flow (Table 3). The minimum value of the average diameter is 21 μm, which is less than the maximum permissible diameter by 4 μm (nozzle #2). Thus, the nozzle with a flow rate of 0.0407 kg/s is the most effective, as it will provide maximum protection of the blade surfaces from drop impact erosion due to a larger number of drops with a diameter of fewer than 25 μm.

Table 3

Comparison of the spraying water effectiveness by a thermopressor with incomplete evaporation

Parameter	Nozzle #1		Nozzle #2		Nozzle #3	
	T_{a1} = 32°C	T_{a1} = 155°C	T_{a1} = 32°C	T_{a1} = 155°C	T_{a1} = 32°C	T_{a1} = 155°C
Consumption of injected water G_w, 10^{-2} kg/s	1.75	1.75	4.07	4.07	4.87	4.87
Minimum supply diameter δ_d.min, μm	25	25	20	15	35	20
Average droplet diameter δ_d.m, μm	39	33	34	21	42	27
The largest number of drops is smaller than the average diameter $< N_\delta$, %	69.4	66.8	66.0	19.4	82.8	69.0
The relative mass of the drops is lower than the average diameter $< m_\delta$, %	18.7	28.5	24.0	34.1	49.0	26.7
The maximum required droplet diameter δ_d.m, μm	25	25	25	25	25	25
The largest number of drops is lower than the maximum required diameter $< N_\delta$, %	39.0	38.5	36.5	49.4	0.0	64.0
The relative mass of the drops is lower than the maximum required diameter $< m_\delta$, %	5.8	12.9	7.1	86.8	0.0	24.7

5. CONCLUSIONS

The use of a thermopressor effect significantly reduces the average droplet diameter of fewer than 25 μm in the dispersed flow due to high turbulence and intensive practically instantaneous evaporation of highly atomized liquid in accelerated superheated air. As a result, a more efficient compression process in the compressor occurs, which makes it possible to compensate for hydraulic pressure losses in the air path with a corresponding reduction in compressive work. It is experimentally determined that the average droplet diameter is significantly reduced to 20–30 μm. The minimum achievable droplet diameter is 15 μm, and the proportion of small drops (less than 25 μm) increases to 40–60%. In addition, the droplet diameter distribution becomes more even, and there are no large droplets with a diameter above 70 μm.

Increasing the water flow during injection positively impacts the number of smaller droplets (around 25 μm), which is advantageous for contact cooling.

Using thermopressor method of cooling compressed air provides maximum protection of blade surfaces from drop-impact erosion, as a consequence of a larger number of droplets with a diameter below 25 μm.

These findings suggest that a thermopressor, when properly configured, can enhance the efficiency of contact cooling systems in gas turbines, leading to improved performance and reliability in power generation applications.

Implementing the insights gained from this research can result in more efficient and reliable gas turbine performance, with reduced wear and erosion of blade surfaces. In addition to gas turbines, the principles explored in this study may have wide applications in marine and stationary power plants based on steam turbines, gas, and internal combustion engines. Improved atomization and cooling techniques can contribute to higher energy conversion efficiency, which is crucial for meeting the growing energy demands while minimizing environmental impacts.

Further research and development can move in the direction of the optimized thermopressor configurations, nozzle designs, and operational parameters to achieve finer droplet sizes and greater control over dispersion.

The widespread adoption of thermopressor-based cooling and atomization technologies has the potential to contribute to environmental sustainability by reducing resource consumption and emissions.

Nomenclature and Units

CHAT	Cascaded Humidified Advanced Turbine
GTE	Gas Turbine Engine
TOPHAT	TOP Humidified Air Turbine

Symbols and units

δ_w	droplet diameter	μm
G_a	air mass flow	kg/s
g_w	relative water amount	%
G_w	water-injected mass flow	kg/s
Ma	Mach number	
T_a	air temperature	°C; K
m_δ	relative mass fraction	%
N_δ	relative number of drops	%

Subscripts

min	minimum
N	number
w	water

REFERENCES

[1] A. Hamdan Al Assaf, A. Amhamed, and O. Fawwaz Alrebei, "State of the art in humidified gas turbine configurations," *Energies*, vol. 15, no. 24, p. 9527, 2022, doi: 10.3390/en15249527.

[2] R. De Robbio, "Micro gas turbine role in distributed generation with renewable energy sources," *Energies*, vol. 16, no. 2, p. 704, 2023, doi: 10.3390/en16020704.

[3] P. Tarnawski and W. Ostapski "Rotating combustion chambers as a key feature of effective timing of turbine engine working according to Humphrey cycle – CFD analysis," *Bull. Pol. Acad. Sci. Tech. Sci.*, vol. 70, no. 5, p. e143100, 2022, doi: 10.24425/bpasts.2022.143100.

[4] O. Mohamed and A. Khalil, "Progress in Modeling and Control of Gas Turbine Power Generation Systems: A Survey," *Energies*, vol. 13, no. 9, p. 2358, 2020, doi: 10.3390/en13092358.

[5] P. Zhu, J.Yao, C. Qian, F. Yang, E. Porpatham, Z. Zhang and Z. Wu, "High-efficiency conversion of natural gas fuel to power by an integrated system of SOFC, HCCI engine, and waste heat recovery: Thermodynamic and thermo-economic analyses," *Fuel,* vol. 275, p. 17883, 2020, doi: 10.1016/j.fuel.2020.117883.

[6] V. Ayhan and Y.M. Ece, "New application to reduce NOx emissions of diesel engines: Electronically controlled direct water injection at compression stroke," *Appl. Energy*, vol. 260, p. 2020, doi: 10.1016/j.apenergy.2019.114328.

[7] A.N. Mustafa, O.M. Ali and O.R. Alomar, "Effect of Heavy Fuel Combustion in a Gas Power Plant on Turbine Performance: A Review," *Int. J. Des. Nat. Ecodyn.*, vol. 17, no. 1, pp. 105–111, 2022, doi: 10.18280/ijdne.170113.

[8] M. Costea and M. Feidt, "A Review Regarding Combined Heat and Power Production and Extensions: Thermodynamic Modelling and Environmental Impact," *Energies*, vol. 15, p. 8782, 2022, doi: 10.3390/en15238782.

[9] M. Kumar, H. Chandra, R. Banchhor, and A. Arora, "Integration of Renewable Energy based Trigeneration Cycle: A Review," *J. Inst. Eng. India Ser. C*, vol. 102, pp. 851–865, 2021, doi: 10.1007/s40032-021-00690-y.

[10] María Isabel Lamas Galdo, "*Marine Engines Performance and Emissions,"* Basel, Switzerland: MDPI, 2021, doi: 10.3390/books978-3-0365-0965-5.

[11] M.K. Wojs, P. Orliński, W. Kamela, and P. Kruczyński, "Research on the influence of ozone dissolved in the fuel-water emulsion on the parameters of the CI engine," in *IOP Conference Series: Materials Science and Engineering,* vol. 148, pp. 1–8, 2016.

[12] V. Kornienko, M. Radchenko, A. Radchenko, H. Koshlak, and R. Radchenko, "Enhancing the Fuel Efficiency of Cogeneration Plants by Fuel Oil Afterburning in Exhaust Gas before Boilers," *Energies*, vol. 16, p. 6743, 2023, doi: 10.3390/en16186743.

[13] N. Radchenko, A. Radchenko, A. Tsoy, D. Mikielewicz, S. Kantor, and V. Tkachenko, "Improving the efficiency of railway conditioners in actual climatic conditions of operation," in *AIP Conf. Proc.,* vol. 2285, p. 030072, 2020, doi: 10.1063/5.0026789.

[14] E.G. Giakoumis, "Turbochargers and turbocharging: Advancements, applications and research," *Nova Science Publishers, Incorporated*, pp. 1–538, 2017, [Online] Available: https://novapublishers.com/shop/turbochargers-and-turbocharging-advancements-applications-and-research.

[15] J.B. Heywood and E. Sher, "*The Two-Stroke cycle engine: Its development, operation and design*," Routledge, 2017, p. 451, doi: 10.1201/9780203734858.

[16] A. Radchenko, N. Radchenko, A. Tsoy, B. Portnoi and S. Kantor, "Increasing the efficiency of gas turbine inlet air cooling in actual climatic conditions of Kazakhstan and Ukraine," in *AIP Conf. Proc.*, vol. 2285, p. 030071, 2020, doi: 10.1063/5.0026787.

[17] M.A. Rahim, "Performance and sensitivity analysis of a combined cycle gas turbine power plant by various inlet air-cooling systems," *Proc. Inst. Mech. Eng. Part A-J. Power Energy*, vol. 226, no. 7, pp. 922–931, 2012.

[18] S. Pourhedayat, E. Hu, and L. Chen, "A comparative and critical review on gas turbine intake air pre-cooling strategies," *Therm. Sci. Eng. Prog.,* vol. 41,p. 101828, 2023, doi: 10.1016/j.tsep.2023.101828.

[19] B. Li, S. Wang, K. Wang, and L. Song, "Thermo-economic analysis of a combined cooling, heating and power system based on carbon dioxide power cycle and absorption chiller for waste heat recovery of gas turbine," *Energy Conv. Manag.*, vol. 224, p.113372, 2020, doi: 10.1016/j.enconman.2020.113372. 2020.

[20] A.M. Pavlenko, "Change of emulsion structure during heating and boiling," *Int. J. Energy Clean Environ.*, vol. 20, pp. 291-302, 2019, doi: 10.1615/InterJEnerCleanEnv.2019032616.

[21] M. Kruzel, T. Bohdal, K. Dutkowski, and M. Radchenko, "The Effect of Microencapsulated PCM Slurry Coolant on the Efficiency of a Shell and Tube Heat Exchanger," *Energies*, vol. 15, no. 4, p. 5142, 2022, doi: 10.3390/en15145142.

[22] G. Chen, V. Ierin, O. Volovyk, and K. Shestopalov, "An improved cascade mechanical compression–ejector cooling cycle," *Energy*, vol. 170, pp. 459-470, 2019, doi: 10.1016/j.energy.2018.12.107.

[23] S. Forduy, A. Radchenko, W. Kuczynski, A. Zubarev, and D. Konovalov, "Enhancing the fuel efficiency of gas engines in integrated energy system by chilling cyclic air," in *International Conference on Advanced Manufacturing Processes. InterPartner-2019. Lecture Notes in Mechanical Engineering*, pp. 500–509, 2020.

[24] R. Radchenko, N. Radchenko, A. Tsoy, S. Forduy, A. Zybarev, and I. Kalinichenko, "Utilizing the heat of gas module by an absorption lithium-bromide chiller with an ejector booster stage". In *AIP Conf. Proc.*, vol. 2285, p. 030084, 2020.

[25] Z. Yang, V. Korobko, M. Radchenko, and R. Radchenko, "Improving Thermoacoustic Low-Temperature Heat Recovery Systems," *Sustainability*, vol. 14, no. 9, p. 12306, 2022.

[26] A. Radchenko, M. Radchenko, D. Mikielewicz, R. Radchenko, and A. Andreev, "A novel degree-hour method for rational design loading," *Proc. Inst. Mech. Eng. Part A-J. Power Energy,* vol. 237, no. 3, pp. 570–579, 2022, doi: 10.1177/09576509221135659.

[27] M. Radchenko *et al.*, "Increasing the Efficiency of Turbine Inlet Air Cooling in Climatic Conditions of China through Rational Designing – Part 1: A Case Study for Subtropical Climate: General Approaches and Criteria," *Energies*, vol. 16, no. 17, p. 6105. 2023, doi: 10.3390/en16176105.

[28] A. Radchenko, I. Scurtu, M. Radchenko, R. Radchenko, S. Forduy, and A. Zubarev, "Monitoring the efficiency of cooling air at the inlet of gas engine in integrated energy system," *Therm. Sci.*, vol. 26, no. 1, pp. 185–194, 2022, doi: 10.2298/TSCI200711344R.

[29] Z. Yang, R. Radchenko, M. Radchenko, A. Radchenko, and V. Kornienko, "Cooling Potential of Ship Engine Intake Air Cooling and Its Realization on the Route Line," *Sustainability*, vol. 14, no. 22, p. 15058, 2022.

[30] H. Aghaali and H.-E. Ångström, "A review of turbocompounding as a waste heat recovery system for internal combustion engines," *Renew. Sust. Energ. Rev.*, vol. 49, pp. 813-824, 2015, doi: 10.1016/j.rser.2015.04.144.

[31] A. Radchenko, M. Radchenko, H. Koshlak, R. Radchenko, and S. Forduy, "Enhancing the Efficiency of Integrated Energy Systems by the Redistribution of Heat Based on Monitoring Data," *Energies*, vol. 15, no. 22, p. 8774, 2022, doi: 10.3390/en15228774.

[32] M. Pan, Y. Huang, Y. Zhu, D. Liang, Y. Liang, and G. Yu, "Co- and trigeneration system based on absorption refrigeration cysle: a review," *Int. J. Green Energy*, vol. 17, no. 14, pp. 912–936, 2020.

[33] M. Radchenko, D. Mikielewicz, A. Andreev, S. Vanyeyev, and O. Savenkov, "Efficient Ship Engine Cyclic Air Cooling by Turboexpander Chiller for Tropical Climatic Conditions," *Lecture Notes in Networks and Systems*, vol. 188, pp. 498–507, 2020.

[34] V. Kornienko, R. Radchenko, M. Radchenko, A. Radchenko, A. Pavlenko, and D. Konovalov, "Cooling Cyclic Air of Marine Engine with Water-Fuel Emulsion Combustion by Exhaust Heat Recovery Chiller," *Energies*, vol. 15, no. 1, p. 248, 2022, doi: 10.3390/en15010248.

[35] K.R. Patel and V.D. Dhiman, "A review on emission and performance of water diesel micro-emulsified mixture-diesel engine," *Int. J. Environ. Sci. Technol,* vol. 19, pp. 8027–8042, 2022.

[36] F. Okumus, G. Kökkülünk, G. Gonca, and I. Kaya, "NO and performance characteristics of a CI engine operated on emulsified fuel," *Int. J. Glob. Warm*, vol. 30, pp. 103–122, 2023.

[37] Z. Yang, V. Kornienko, M. Radchenko, A. Radchenko, R. Radchenko, and A. Pavlenko, "Capture of pollutants from exhaust gases by low-temperature heating surfaces," *Energies*, vol. 15, no. 1, p. 120, 2022, doi: 10.3390/en15010120.

[38] Z. Yang, V. Kornienko, M. Radchenko, A. Radchenko, and R. Radchenko, "Research of Exhaust Gas Boiler Heat Exchange Surfaces with Reduced Corrosion When Water-Fuel Emulsion Combustion," *Sustainability*, vol. 14, no. 19, p. 11927, 2022.

[39] N. Gandhi and S. Suresh, "Effect of mist concentration on the cooling effectiveness of a diffused hole mist cooling system," *J. Therm. Anal. Calorim.*, vol. 141, pp. 2231–2238, 2020, doi: 10.1007/s10973-020-09680-1.

[40] Z. Yang, M. Radchenko, A. Radchenko, D. Mikielewicz, and R. Radchenko, "Gas Turbine Intake Air Hybrid Cooling Systems and a New Approach to Their Rational Designing," *Energies*, vol. 15, no. 4, p. 1474, 2022, doi: 10.3390/en15041474.

[41] A. Radchenko, M. Radchenko, D. Mikielewicz, A. Pavlenko, R. Radchenko, and S. Forduy, "Energy Saving in Trigeneration Plant for Food Industries," *Energies*, vol. 15, no. 3, p. 1163, 2022, doi: 10.3390/en15031163.

[42] A. Fowle, *An experimental investigation of an aerothermopressor having a gas flow capacity of 25 pounds per second*, Massachusetts Institute of Technology, 1972.

[43] M.T. Mito, M.A. Teamah, W.M. El-Maghlany, and A.I. Shehata, "Utilizing the scavenge air cooling in improving the per-formance of marine diesel engine waste heat recovery systems," *Energy*, vol. 142, pp. 264–276, 2018, doi: 10.1016/j.energy.2017.10.039.

[44] Z. Yu *et al*., "Investigation of Thermopressor with Incomplete Evaporation for Gas Turbine Intercooling Systems" *Energies*, vol. 16, no. 1, p. 20, 2023.

[45] D. Konovalov, E. Trushliakov, M. Radchenko, H. Kobalava, and V. Maksymov, "Research of the aerothermopressor cooling system of charge air of a marine internal combustion engine under variable climatic conditions of operation," *Lecture Notes in Mechanical Engineering*, pp. 520–529, 2020.

[46] N.I. Radchenko, "On reducing the size of liquid separators for injector circulation plate freezers," *Int. J. Refrig.*, vol. 8, pp. 267–269. 1985.

[47] N.A. Radchenko, "Concept of the design and operation of heat exchangers with change of phase," *Arch.Thermodyn.,* vol. 25, pp. 3-18. 2004.

[48] S. Serbin, M. Radchenko, A. Pavlenko, K. Burunsuz, A. Radchenko, and D. Chen, "Improving Ecological Efficiency of Gas Turbine Power System by Combusting Hydrogen and Hydrogen-Natural Gas Mixtures," *Energies*, vol. 16, no. 9, p. 3618, 2023, doi: 10.3390/en16093618.

[49] A.M. Pavlenko and H. Koshlak, "Application of Thermal and Cavitation Effects for Heat and Mass Transfer Process Intensification in Multicomponent Liquid Media," *Energies*, vol. 14, no. 23, p. 7996, 2021, doi: 10.3390/en14237996.

[50] M. Radchenko, A. Radchenko, E. Trushliakov, A. Pavlenko, and R. Radchenko, "Advanced Method of Variable Refrigerant Flow (VRF) Systems Designing to Forecast On-Site Operation – Part 1: General Approaches and Criteria," *Energies*, vol. 16, no. 3, p. 1381, 2023, doi: 10.3390/en16031381.

[51] M. Radchenko, A. Radchenko, E. Trushliakov, H. Koshlak, and R. Radchenko, "Advanced method of variable refrigerant flow (VRF) systems designing to forecast on site operation. Part 2: Phenomenological simulation to recuperate refrigeration energy," *Energies*, vol. 16, no. 3, p. 1922, 2023, doi: 10.3390/en16041922.

[52] M. Radchenko, A. Radchenko, E. Trushliakov, A. Pavlenko, and R. Radchenko, "Advanced Method of Variable Refrigerant Flow (VRF) System Design to Forecast on Site Operation – Part 3: Optimal Solutions to Minimize Sizes," *Energies*, vol. 16, no. 5, p. 2417, 2023, doi: 10.3390/en16052417.

[53] D. Konovalov *et al.*, "Recent Developments in Cooling Systems and Cooling Management for Electric Motors," *Energies*, vol. 16, no. 19, p. 7006, 2023, doi: 10.3390/en16197006.

[54] M. Chaker and C. Meher-Homji, "Inlet fogging of gas turbine engines: climatic analysis of gas turbine evaporative cooling potential of international locations," in Proc. *ASME Turbo Expo 2002*, The Netherlands, 3-6 June 2002, p. GT-2002-30559, 2002, doi: 10.1115/GT2002-30559.

[55] M. Chaker, C.B. Meher-Homji, T. Mee, and A. Nicolson, "Inlet fogging of gas turbine engines- detailed climatic analysis of gas turbine evaporative cooling potential," *ASME International Gas Turbine and Aeroengine Conference*, USA, 4–7 June 2001, p. GT-526, 2001.

[56] P. Barabash, A. Solomakha, and V. Sereda, "Experimental investigation of heat and mass transfer characteristics in direct contact exchanger," *Int. J. Heat Mass Transf.*, vol. 162, p. 120359, 2020, doi: 10.1016/j.ijheatmasstransfer.2020.120359.

[57] L. Zhao and T. Wang, "An experimental study of Mist/Air film cooling on a flat plate with application to gas turbine airfoils - Part 2: Two-phase flow measurements and droplet dynamics," in Proc. *ASME Turbo Expo 2013*, 2013, p. GT2013-94478.

[58] K. Shukla, A. Sharma, M. Sharma, and S. Mishra, "Performance Improvement of Simple Gas Turbine Cycle with Vapor Compression Inlet Air Cooling," *Mater. Today-Proc.*, vol. 5, pp. 19172-19180, 2018, doi: 10.1016/j.matpr.2018.06.272.

[59] M. Chaker, C.B. Meher-Homji, and T. Mee, III, "Inlet fogging of gas turbine engines – Part I: Fog droplet thermodynamics, heat transfer, and practical considerations," *J. Eng. Gas Turbines Power*, vol. 126, pp. 545–558, 2004, doi: 10.1115/1.1712981.

[60] K. Dutkowski and M. Kruzel, "Microencapsulated PCM slurries' dynamic viscosity experimental investigation and temperature-dependent prediction model," *Int. J. Heat Mass Transf.*, vol. 145, p. 118741, 2019, doi: 10.1016/j.ijheatmasstransfer.2019.118741.

[61] A.K. El-Fiqi, N.H. Ali, H.T. El-Dessouky, H.S. Fath, and M.A. El-Hefni, "Flash evaporation in a superheated water liquid jet," *Desalination*, vol. 206, no. 1–3, pp. 311–321, 2007, doi: 10.1016/j.desal.2006.05.017.

[62] M. Dikij, A. Solomaha, and V. Petrenko, "Mathematical model of water droplets evaporation in air stream," *East.-Europ. J. Enterp. Technol.*, vol. 3, no. 10, p. 63–68, 2013.

[63] M. Dikij and A. Solomaha, "Experimental investigation of superheated water atomization," *East.-Europ. J. Enterp. Technol*, vol. 8, no. 61, pp. 20–25, 2013.

[64] A.A. Dolinsky and A. Solomaha, *Direct cooling cyclic air process features in gas turbine engine and method for it realization Energy: economics, technology, ecology*, National Technical University of Ukraine Kyiv Polytechnic Institute, pp. 22–27, 2012.

[65] A. Dolinsky, M. Kovetskaya, A. Skitsko, A. Avramenko, and B. Basok, "Nonstationary heat transfer crisis in annular dispersed flows," *J. Eng. Thermophys.*, no. 17, pp. 126–129, 2008, doi: 10.1134/S1810232808020045.

[66] A. Naeim Khaled, A.A. Hegazi , M.M. Awad, and S.H. El-Emam. "Inlet air fogging strategy using natural gas fuel cooling potential for gas turbine power plants," *Case Stud. Therm. Eng.*, vol. 37, p. 102235, 2022, doi: 10.1016/j.csite.2022.102235.

[67] N. Kapilan, A.M. Isloor, and S. Karinka, "Inlet Fogging of Gas Turbine Engines: Climatic Analysis of Gas Turbine," *Results Eng.*, vol. 18, p. 101059, 2023, doi: 10.1016/j.rineng.

[68] M. Chaker and T.R. Mee, "Design consideration of fogging and wet compression systems as function of gas turbine inlet duct configurations," in Proc. *ASME Turbo Expo 2015*, 2015, p. GT2015-43229.

[69] P. Redding, J. Crutcher, J. Gabriel, P. Bruner, C. Meher-Homji, D. Messersmith, B. Barnes and K. Masani, "World's first application of gas turbine inlet air chilling for LNG liquefaction - Design, implementation and operation," in Proc. *18th International Conference and Exhibition on Liquefied Natural Gas 2016, LNG 2016*, 2016, pp. 857–872.

[70] M. Chaker and C.B. Meher-Homji, "Evaporative Cooling of Gas Turbine Engines," *J. Eng. Gas. Turbines Power*, vol. 135, no. 8, p. 081901, 2013, doi: 10.1115/1.4023939.

[71] V. Kornienko, R. Radchenko, T. Bohdal, M. Radchenko, and A. Andreev, "Thermal Characteristics of the Wet Pollution Layer on Condensing Heating Surfaces of Exhaust Gas Boilers," *Lecture Notes in Mechanical Engineering*, pp. 339–348, 2021.

[72] S. Jolly, S. Cloyd, and J. Hinrichs, "Wet compression adds power, flexibility to aeroderivative GTs," *Power*, vol. 149, pp. 52–57, 2005.

[73] J. Van Liere and G.H.M. Laagland, "The tophat® cycle," *VDI Berichte*, 2000, pp. 161–175.

[74] H.M. Kwon, T.S. Kim, and J.L. Sohn, "Performance improvement of gas turbine combined cycle power plant by dual cooling of the inlet air and turbine coolant using an absorption chiller," *Energy*, vol.163, pp. 1050–1061, 2018, doi: 10.1016/j.energy.2018.08.191.

[75] H.A. Al-Ansary, J.A. Orfi, and M.E. Ali, "Impact of the use of a hybrid turbine inlet air cooling system in arid climates," *Energy Conv. Manag.*, vol. 75, pp. 214–223, 2013, doi: 10.1016/j.enconman.2013.06.005.

[76] D.A. Block Novelo, U. Igie, V. Prakash, and A. Szymański, "Experimental investigation of gas turbine compressor water injection for NOx emission reductions," *Energy*, vol. 176, pp. 235–248, 2019, doi: 10.1016/j.energy.2019.03.187.

[77] A. Suryan, D.S. Kim, and H.D. Kim, "Experimental study on the inlet fogging system using two-fluid nozzles," *J. Therm. Sci.*, no. 19, pp. 132–135, 2010, doi: 10.1007/s11630-010-0132-3.

[78] A.K. Shukla and O. Singh, "Impact of inlet fogging on the performance of Steam injected cooled gas turbine based combined cycle power plant," in Proc. *ASME 2017 Gas Turbine India Conference. Volume 1: Compressors, Fans and Pumps; Turbines; Heat Transfer; Combustion, Fuels and Emissions*, India, 2017, doi: 10.1115/GTINDIA2017-4557.

[79] R. Abdelmaksoud and T. Wang, "A Numerical Investigation of Air/Mist Cooling Through a Conjugate, Rotating 3D Gas Turbine Blade With Internal, External, and Tip Cooling," *J. Therm. Sci. Eng. Appl.*, vol. 13, no. 2, p. 021004, 2020, doi: 10.1115/1.4047279.

[80] A. Mohan, A. Suryan, D.H. Doh, and H.D. Kim, "Thermo-fluid dynamics of the effects of water spray on air compression process," in Proc. *12th European Conference on Turbomachinery Fluid Dynamics and Thermodynamics, ETC 2017*, 2017. doi: 10.29008/etc2017-104.

[81] M.P. Boyce, *Gas Turbine Engineering Handbook*. Gulf Professional Publishing, 2017, p. 816.

[82] A. Radchenko, D. Mikielewicz, S. Forduy, M. Radchenko, and A. Zubarev, "Monitoring the Fuel Efficiency of Gas Engine in Integrated Energy System," in Proc. *Advances in Intelligent Systems and Computing*, 2020, vol. 1113 pp. 361–370.

[83] N. Patel, M. Modi and T. Patel, "Investigation of diesel engine with water emulsifier - A review," *Int. Res. J. Eng. Technol.*, vol. 4, no. 2, pp. 879–883, 2017.

[84] N. Radchenko, E. Trushliakov, A. Radchenko, A. Tsoy, and O. Shchesiuk, "Methods to determine a design cooling capacity of ambient air conditioning systems in climatic conditions of Ukraine and Kazakhstan," in *AIP Conf. Proc.*, vol. 2285, p. 030074, 2020, doi: 10.1063/5.0026790.

[85] A. Radchenko, M. Radchenko, E. Trushliakov, S. Kantor, and V. Tkachenko, "Statistical Method to Define Rational Heat Loads on Railway Air Conditioning System for Changeable Climatic Conditions," in Proc. *5th International Conference on Systems and Informatics, ICSAI 2018*, China, 2018, pp. 1294–1298.

[86] D. Konovalov *et al.*, "Research of characteristics of the flow part of an aerothermopressor for gas turbine intercooling air. Proceedings of the Institution of Mechanical Engineers, Part A," *Proc. Inst. Mech. Eng. Part A-J. Power Energy*, vol. 236, pp. 634–646, 2022, doi: 10.1177/09576509211057952.

[87] G. Chen, V. Zhelezny, O. Khliyeva, K. Shestopalov, and V. Ierin, "Ecological and energy efficiency analysis of ejector and vapor compression air conditioners," *Int. J. Refrig.*, vol. 74, pp. 129–137, 2017, doi: 10.1016/j.ijrefrig.2016.09.028.

[88] D. Konovalov *et al.*, "Recent Developments in Cooling Systems and Cooling Management for Electric Motors," *Energies*, vol. 16, no. 19, p. 7006, 2023, doi: 10.3390/en16197006.

[89] Z. Yang *et al.*, "Analysis of Efficiency of Thermopressor Application for Internal Combustion Engine," *Energies*, vol. 15, no. 6, p. 2250, 2022, doi: 10.3390/en15062250.